GeoScienceWorld
Lithosphere
Volume 2023, Article ID lithosphere_2023_153, 7 pages
https://doi.org/10.2113/2023/lithosphere_2023_153

Lithosphere

Research Article

A Novel Method to Predict the Permeability of Heterogeneous Sandstones Using Multiple Echo Spacing NMR Measurements

Yufeng Xiao,[1,2] Hongyan Wang,[2] Zhenxue Jiang,[1] Xinmin Ge,[3] Renxia Zhang,[3] Fangle Song,[4] and Jianyu Liu[5]

[1]*Unconventional Petroleum Research Institute, China University of Petroleum, Beijing, China*
[2]*Petrochina Research Institute of Petroleum Exploration and Development, Beijing, China*
[3]*School of Geosciences, China University of Petroleum, Qingdao, China*
[4]*College of Geoscience, China University of Petroleum, Beijing, China*
[5]*PetroChina Research Institute of Petroleum Exploration and Development, Northwest Branch, Lanzhou, China*

Correspondence should be addressed to Hongyan Wang; wanghongyan69@petrochina.com.cn

Received 23 March 2023; Published 15 December 2023

Academic Editor: Chen Guo

We propose a novel method for estimating the permeability of heterogeneous sandstones based on the nuclear magnetic resonance (NMR) data with multiple echo spacings. The decaying curves and their corresponding spectra are obtained for different echo spacings to investigate the relaxation property, the diffusion term, and the signal loss contributed by higher echo spacing. Moreover, an empirical model is developed to correlate permeability with the differential decay rate. The result shows that the geometric transversal relaxation time is positively related to echo spacing, which disobeys the traditional cognition. Moreover, the absolute value of the differential decay rate is positively correlated with the echo spacing and exhibits a power law behavior. More interestingly, it is observed that the permeability diminishes in a power law behavior with respect to fitting parameters. This marks the first attempt to establish a relationship between the permeability and NMR data with different echo spacings, which is hopeful to be extended to other complex reservoirs with the availability of multiple echo spacing data.

1. Introduction

The low-field nuclear magnetic resonance (NMR) technique acts as an important tool in petroleum and geological studies. Compared with other geophysical data, the signal originates from hydrogen and provides valuable lithology-independent information such as pore size, porosity, permeability, fluid saturation, viscosity, as well as wettability [1–3]. The transversal relaxation time (T_2) generated by the Carr-Purcell-Meiboom-Gill pulse sequence is the most frequently used parameter nowadays. Over the past few decades, there have been tremendous examples of permeability estimation using NMR data such as the Schlumberger-Doll Research equation and the Timur-Coates equation. Although both equations provide a trend in permeability prediction, their shortcomings are obvious and they are demonstrated to have large errors in complex reservoirs such as carbonate, tight sand, shale, and mudstone [4–9]. The most widely used and improved permeability models are based on the two well-known equations incorporating the rock typing strategy, multiple regressions, and combination with other geophysical data [10–14]. Some models adopting the transformation of T_2 and raw decaying signals are also reported to achieve favorable results [5].

However, the precision of these models is strongly dependent on the accuracy of the NMR data. It is recognized that the NMR measurement can be easily distorted due to inadequate signal acquisition, low signal-to-noise

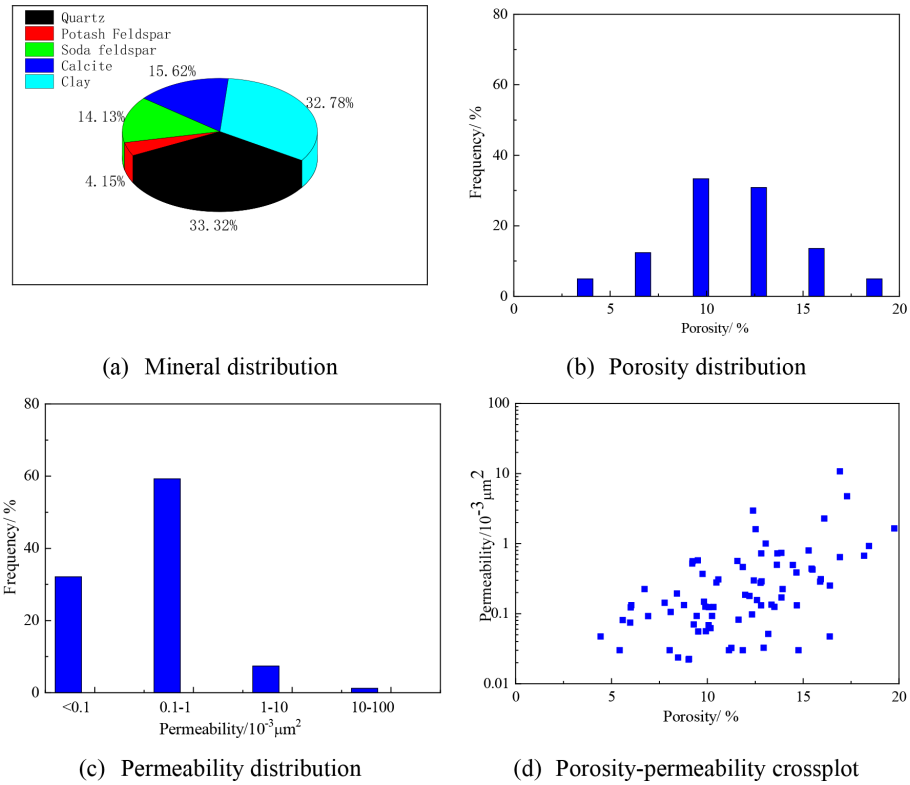

(a) Mineral distribution (b) Porosity distribution

(c) Permeability distribution (d) Porosity-permeability crossplot

Figure 1: General lithology and reservoir property of the studied area.

ratio, inaccurate inversion algorithm, as well as the presence of paramagnetic materials [15, 16], resulting in an unreliable result.

This work discusses the NMR relaxation of the heterogeneous sandstone with different echo spacings to investigate the correlation between the permeability and the differential decay rate, aiming to propose a novel method for predicting the permeability. The rest of the paper is organized as follows. In Section 2, we describe the NMR theory and the experimental procedure. In Section 3, we analyzed the NMR responses at different echo spacings and proposed a novel model. We provide the conclusion and discussion in the last section.

2. Theory and Experiment

According to the NMR principle, the transversal relaxation time of the porous media is expressed as [2],

$$\frac{1}{T_2}=\frac{1}{T_{2s}}+\frac{1}{T_{2b}}+\frac{1}{T_{2d}}=\rho_2\frac{S}{V}+\frac{1}{T_{2b}}+\frac{D(G\gamma T_E)^2}{12} \quad (1)$$

where T_{2s}, T_{2b}, and T_{2d} represent the surface transverse relaxation time, the bulk transverse relaxation time, and the diffusion transverse relaxation time, respectively. S is the surface area of pore space, V is the pore volume, ρ_2 is the transversal surface relaxivity, D is the diffusion coefficient, γ is the gyromagnetic ratio, T_E is the echo spacing, and G is the magnetic field gradient.

In many studies, bulk and diffusion relaxations are often neglected. Consequently, the transversal relaxation time can be expressed as [2],

$$\frac{1}{T_2}=\frac{1}{T_{2s}}=\rho_2\frac{S}{V}=\rho_2\frac{F_s}{r} \quad (2)$$

where F_s is the pore shape factor and r is the pore radius.

Most pore structure evaluation methods and permeability models are based on the above assumption. However, the diffusion term cannot be ignored when the internal gradient is strong or the echo spacing is large, particularly in volcanic and shale reservoirs [17–19].

For well-defined porous media with a single intrinsic relaxation time, the differential decay rate between two different echo spacings is stated as [20],

$$\nabla\frac{1}{T_2}=\frac{1}{T_{2El}}-\frac{1}{T_{2Es}}=\frac{DG^2\gamma^2\left(T_{El}^2-T_{Es}^2\right)}{12} \quad (3)$$

where T_{El} and T_{Es} represent the long and short echo spacings, respectively, and T_{2El} and T_{2Es} are the geometric transversal relaxation time of the long and short echo spacings.

The echo signal inverse problem can be transformed into a linear equation-solving problem:

$$y=Ax+\varepsilon \quad (4)$$

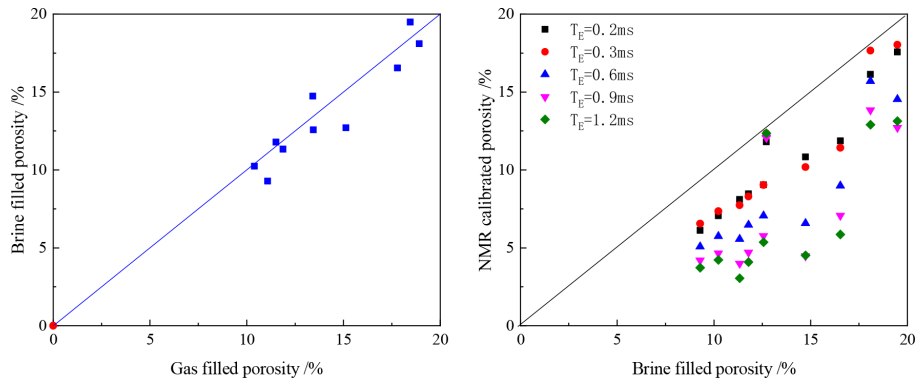

(a) Gas porosity and brine filled porosity (b) Brine filled porosity and NMR porosity

FIGURE 2: Comparisons among the porosity measured with different methods.

where y is the measured echo signal; $A = \exp(-t/T_2)$; ε is the error; and x is the vector to be solved.

The formula obtained after regularization [21, 22]:

$$x_\alpha = \operatorname{argmin}\left\{\|Ax - y\|_2^2 + \alpha^2\|Lx\|_2^2\right\} \tag{5}$$

where α is the regularization parameter and L matrix is the regularization operator.

The studied area is located in the eastern segment of Alkin Piedmont, Qaidam Basin, western China. Figure 1(a) presents the mineral distributions from the X-ray diffraction analysis. It is shown that the main constitutes are quartz and clay. Figure 1(b) and Figure 1(c) represent the frequency distributions of gas porosity and gas permeability, indicating that the reservoir property is poor. Figure 1(d) shows the crossplot of the porosity and the permeability for typical samples. It is obvious that the relationship between the porosity and the permeability is scattered, indicating high heterogeneity.

Ten core samples were selected to conduct NMR experiments. After the necessary pretreatments, the gas porosity and steady-state permeability were measured first. Then, we used a 2 MHz NMR benchtop developed by the NIUMAG Corporation to detect the relaxation signals of brine-saturated samples. The detailed experimental procedure was elaborated in our previous publications [23]. The NMR acquisition parameters are as follows: the number of scans is 50, the waiting time is 6 seconds, the receiving gain is 80%, and the echo spacing series are 0.2 ms, 0.3 ms, 0.6 ms, 0.9 ms, and 1.2 ms, respectively.

3. Results and Analysis

Figure 2(a) shows the comparison between the gas porosity and the brine-filled porosity. It is seen that the porosity measured by both methods is equivalent. A slight deviation is attributed to the experimental error. Figure 2(b) depicts the relationship between the brine-filled porosity and the NMR porosity at different echo spacings. Generally, the NMR porosity is lower than the brine-filled porosity. The phenomenon reveals that the porosity is underestimated by NMR measurements, which may be contributed by the fast relaxation components or other factors. In addition, the NMR porosity is generally inversely proportional to the echo spacing [20, 24]. However, each sample has its unique deviation trend with the echo spacing.

Figure 3 represents the T_2 spectra measured at different echo spacings for brine-saturated samples. It is seen that the amplitude is also inversely proportional to the echo spacing but with different trends. More interestingly, substantial signal losses are observed for samples with high echo spacing, indicating the insufficient acquisition of fast relaxation components.

$$T_{2,mean} = \frac{\sum f_i T_{2i}}{\sum f_i} \tag{6}$$

Where $T_{2,mean}$ is the geometric T_2 mean; T_{2i} is the ith T_2 relaxation; and f_i is the amplitude of the ith T_2 relaxation component.

It is obvious from Figure 4(a) that the geometric T_2 mean is positively correlated with the echo spacing. Consequently, a negative differential decay rate is observed, as shown in Figure 4(b). The possible reason may be that the influence of the signal loss caused by the echo spacing is more distinct than the diffusional relaxation induced by the internal gradient. The phenomenon is of great importance for petrophysicists, and special precautions should be taken when using the NMR data for formation evaluation. Moreover, the power function can be used to describe the relationship between the differential decay rate and the echo spacing, which is expressed as,

$$\left(-\nabla\frac{1}{T_2}\right) = AT_E^B \tag{7}$$

where A and B are fitting parameters.

Figure 4(c) and 4(d) show the relationship between the permeability and the above two fitting parameters. Interestingly, it is observed that the permeability exponentially decays with A, which is expressed by,

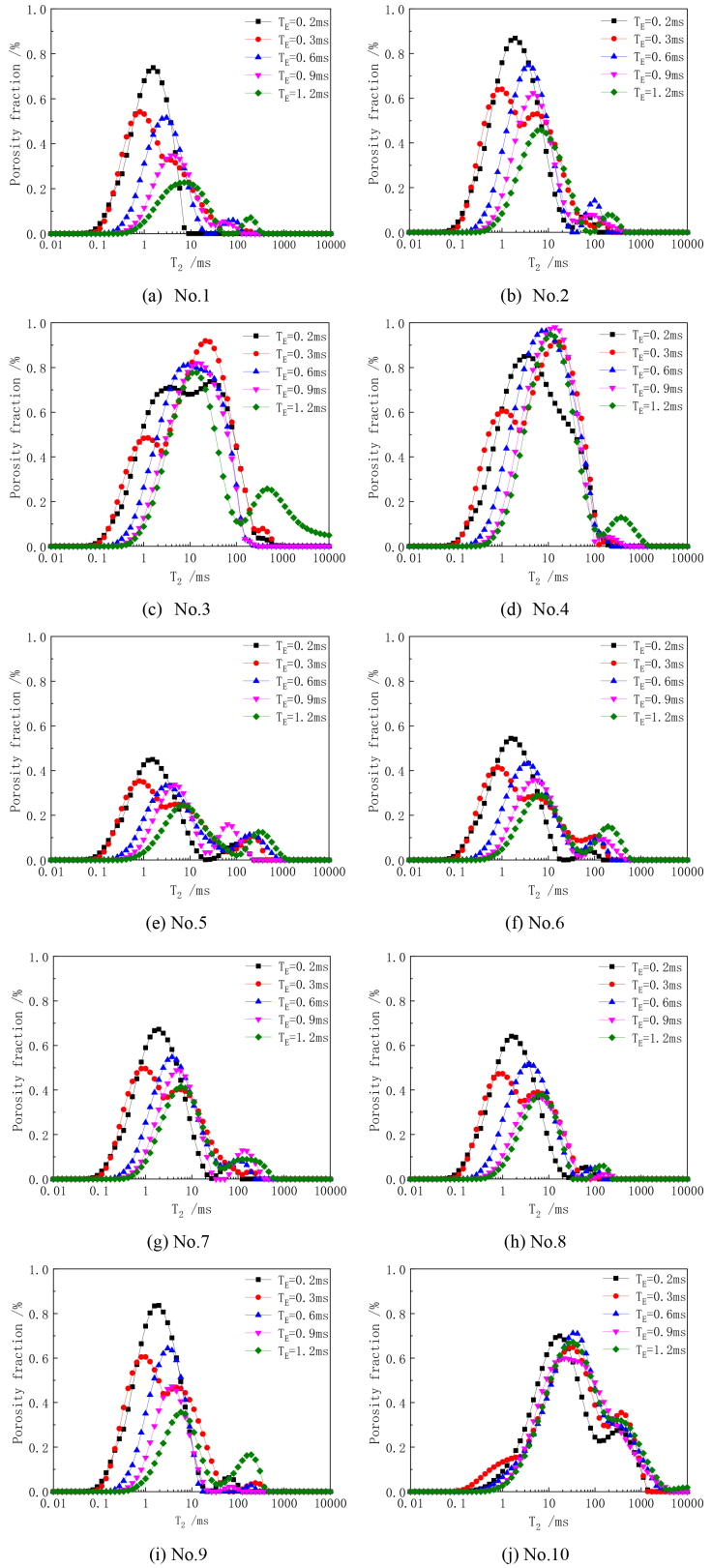

FIGURE 3: NMR T_2 spectra of brine-saturated samples at different echo spacings.

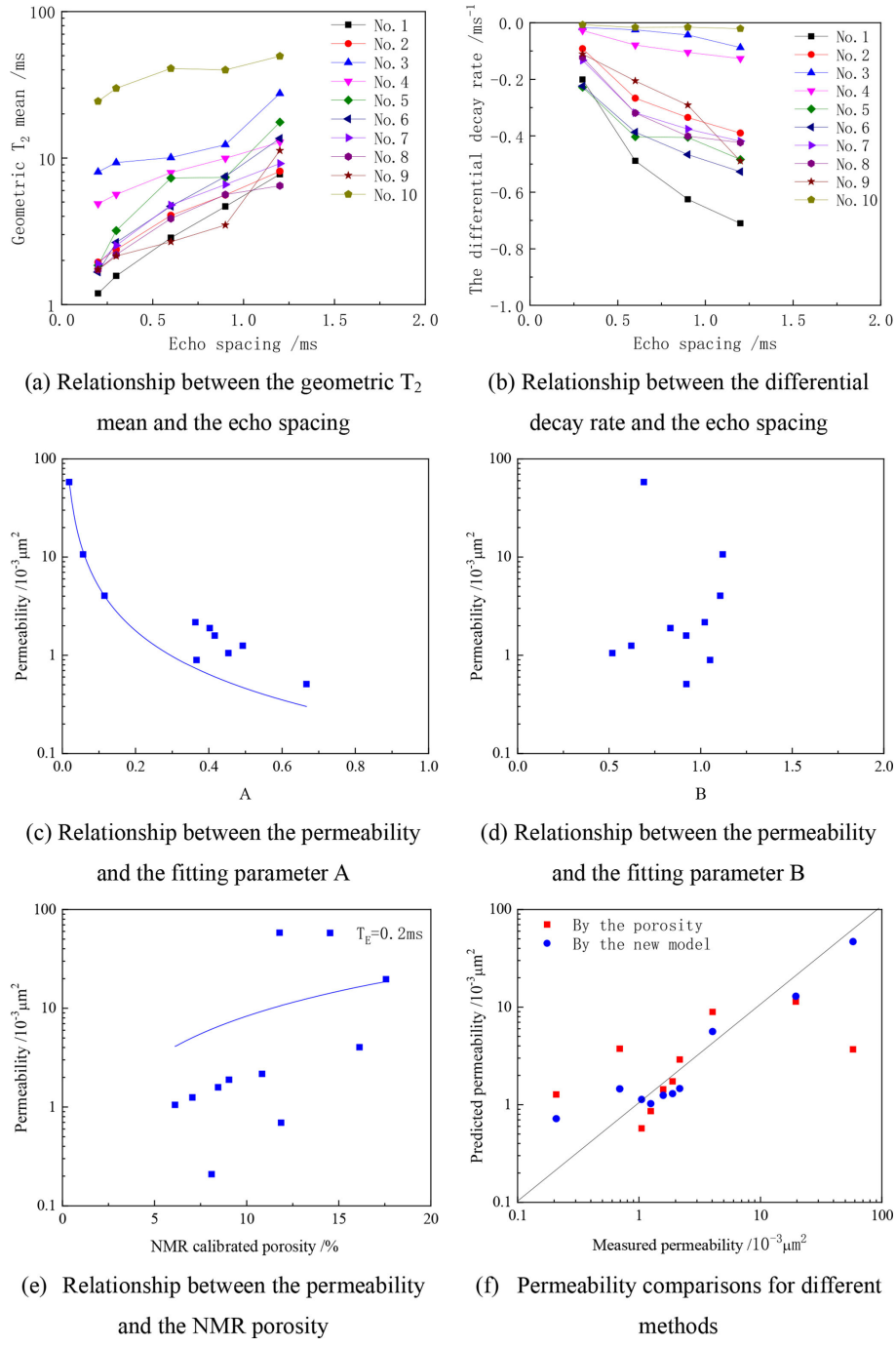

(a) Relationship between the geometric T_2 mean and the echo spacing

(b) Relationship between the differential decay rate and the echo spacing

(c) Relationship between the permeability and the fitting parameter A

(d) Relationship between the permeability and the fitting parameter B

(e) Relationship between the permeability and the NMR porosity

(f) Permeability comparisons for different methods

Figure 4: NMR T_2 spectra of brine-saturated samples at different echo spacings.

$$K = cA^{-d} = c\left(\frac{\log\left(-\nabla\frac{1}{T_2}\right)}{B\log(T_E)}\right)^{-d} \quad (8)$$

where K is the permeability and c and d are fitting parameters. In this study, they are 0.447 and 1.172, respectively. The correlation coefficient is 0.946.

Meanwhile, the conventional porosity-permeability crossplot is also implemented to fit permeability, as is shown in Figure 4(e). It is obvious that the correlation is poor. Figure 4(f) compares the predicted permeability and the measured permeability for all core samples. It is seen that the NMR-based permeability achieves higher reliability compared with the regression of the porosity although the theoretical fundamentals are not known.

4. Conclusions

Based on NMR measurements of heterogeneous sandstone samples at different echo spacings, we have reached the following conclusions:

(1) The echo spacing has a significant influence on NMR signals. Both the NMR porosity and the amplitude of T_2 spectra are inversely proportional to the echo spacing.

(2) The differential decay rate is negatively correlated with the echo spacing, indicating that the influence of the echo spacing is larger than the internal gradient.

(3) The permeability is strongly correlated with the fitting parameter, and a power law behavior was observed between the absolute differential decay rate and the echo spacing.

(4) The proposed permeability utilizing multiple echo spacing NMR data achieves favorable results compared with the conventional porosity-permeability crossplot model.

However, much work should be done to extend this model to field applications and other complex reservoirs. The theoretical fundamentals and the intrinsic mechanism of the relationship between the permeability and the echo spacing should be further investigated.

Data Availability

The data that support the findings of this study are available on request from the corresponding author. The data are not publicly available due to privacy restrictions.

Conflicts of Interest

The authors declare that they have no conflicts of interest.

Acknowledgments

This work was supported by the CNPC Innovation Fund (2021DQ02-0402), the Natural Science Foundation of Shandong Province (ZR2023YQ034), and the National Natural Science Foundation of China (42174142).

References

[1] G. R. Coates, L. Z. Xiao, and M. G. Prammer, *NMR Logging: Principles and Applications*, Haliburton Energy Services, Houston, 1999.

[2] K. J. Dunn, D. J. Bergman, and G. A. LaTorraca, *Nuclear Magnetic Resonance: Petrophysical and Logging Applications*. 2 Eds, Elsevier, 2002.

[3] R. Freedman, N. Heaton, M. Flaum, G. J. Hirasaki, C. Flaum, and M. Hürlimann, "Wettability, saturation, and viscosity from NMR measurements," *SPE Journal*, vol. 8, no. 4, pp. 317–327, 2003.

[4] H. Daigle and B. Dugan, "Extending NMR data for permeability estimation in fine-grained sediments," *Marine and Petroleum Geology*, vol. 26, no. 8, pp. 1419–1427, 2009.

[5] R. Rezaee, A. Saeedi, and B. Clennell, "Tight gas sands permeability estimation from mercury injection capillary pressure and nuclear magnetic resonance data," *Journal of Petroleum Science and Engineering*, vols. 88–89, pp. 92–99, 2012.

[6] K. Dlubac, R. Knight, Y. Song, et al., "Use of NMR logging to obtain estimates of Hydraulic conductivity in the high plains Aquifer," *Water Resources Research*, vol. 49, no. 4, pp. 1871–1886, 2013. https://agupubs.onlinelibrary.wiley.com/toc/19447973/49/4.

[7] X. Ge, Y. Fan, J. Liu, L. Zhang, Y. Han, and D. Xing, "An improved method for permeability estimation of the Bioclastic limestone reservoir based on NMR data," *Journal of Magnetic Resonance*, vol. 283, pp. 96–109, 2017.

[8] H. E. Mason, M. M. Smith, and S. A. Carroll, "Calibration of NMR porosity to estimate permeability in carbonate reservoirs," *International Journal of Greenhouse Gas Control*, vol. 87, pp. 19–26, 2019.

[9] Y. Fan, J. Liu, X. Ge, S. Deng, H. Liu, and D. Gu, "Permeability evaluation of tight Sandstone based on dual T2 cutoff values measured by NMR," *Chinese Journal of Geophysics*, vol. 61, no. 4, pp. 1628–1638, 2018.

[10] H. Westphal, I. Surholt, C. Kiesl, H. F. Thern, and T. Kruspe, "NMR measurements in carbonate rocks: problems and an approach to a solution," *Pure and Applied Geophysics PAGEOPH*, vol. 162, no. 3, pp. 549–570, 2005.

[11] E. H. Rios, I. Figueiredo, A. K. Moss, et al., "NMR permeability Estimators in 'Chalk'Carbonate rocks obtained under different relaxation times and MICP size Scalings," *Geophysical Journal International*, vol. 206, no. 1, pp. 260–274, 2016.

[12] J. Cai, D. Lin, H. Singh, S. Zhou, Q. Meng, and Q. Zhang, "A simple permeability model for shale gas and key insights on relative importance of various transport mechanisms," *Fuel*, vol. 252, pp. 210–219, 2019.

[13] F. Razavirad, M. Schmutz, and A. Binley, "Estimation of the permeability of hydrocarbon reservoir samples using induced polarization and nuclear magnetic resonance methods," *Geophysics*, vol. 84, no. 2, pp. MR73–MR84, 2019.

[14] W. Yan, J. Sun, H. Dong, and L. Cui, "Investigating NMR-based absolute and relative permeability models of Sandstone using Digital rock techniques," *Journal of Petroleum Science and Engineering*, vol. 207, p. 109105, 2021.

[15] V. Anand and G. J. Hirasaki, "Paramagnetic relaxation in Sandstones: distinguishing T1 and T2 dependence on surface relaxation, internal gradients and dependence on echo spacing," *Journal of Magnetic Resonance*, vol. 190, no. 1, pp. 68–85, 2008.

[16] M. N. Testamanti and R. Rezaee, "Considerations for the acquisition and inversion of NMR T_2 data in Shales," *Journal of Petroleum Science and Engineering*, vol. 174, pp. 177–188, 2019.

[17] G. Q. Zhang, G. J. Hirasaki, and W. V. House, "Effect of internal field gradients on NMR measurements," *Petrophysics*, vol. 42, no. 1, pp. 37–47, 2001.

[18] E. L. Fay, D. J. Grombacher, and R. J. Knight, "Investigating the effect of internal gradients on static gradient nuclear magnetic resonance diffusion measurements," *Geophysics*, vol. 82, no. 5, pp. D293–D301, 2017.

[19] D. Xing, Y. Fan, S. Deng, X. Ge, J. Liu, and F. Wu, "Influential factors of internal magnetic field gradient in reservoir rock and its effects on NMR response," *Applied Magnetic Resonance*, vol. 49, no. 3, pp. 227–237, 2018.

[20] X. Ge, J. Zhao, F. Zhang, et al, "A practical method to compensate the effect of echo spacing on the shale NMR T_2 spectrum," *Earth and Space Science*, vol. 6, no. 8, pp. 1489–1497, 2019.

[21] Y.-L. Zou, R.-H. Xie, and A. Arad, "A numerical estimation of choice of the Regularization parameter for NMR T2 inversion," *Petroleum Science*, vol. 13, no. 2, pp. 237–246, 2016.

[22] G. Luo, L. Xiao, S. Luo, G. Liao, and R. Shao, "A study on multi-exponential inversion of nuclear magnetic resonance relaxation data using deep learning," *Journal of Magnetic Resonance*, vol. 346, p. 107358, 2023.

[23] X. Ge, Y. Fan, X. Zhu, Y. Chen, and R. Li, "Determination of nuclear magnetic resonance T_2 cutoff value based on Multifractal theory-an application in Sandstone with complex pore structure," *GEOPHYSICS*, vol. 80, no. 1, pp. D11–D21, 2015.

[24] B. Min, C. H. Sondergeld, and C. S. Rai, "Investigation of high frequency 1D NMR to characterize reservoir rocks," *Journal of Petroleum Science and Engineering*, vol. 176, pp. 653–660, 2019.